

DIGITAL RECEIVER FOR TR-UWB SYSTEMS WITH INTER-PULSE INTERFERENCE

Jin Tang, Zhengyuan Xu

Department of Electrical Engineering
University of California
Riverside, CA 92521
{jtang,dxu}@ee.ucr.edu

Brian M. Sadler

Army Research Laboratory
AMSRL-CI-CN
Adelphi, MD 20783
bsadler@arl.army.mil

ABSTRACT

An ultra wideband (UWB) transmitted reference (TR) system that allows inter-pulse interference (IPI) was recently proposed. It relaxes a restrictive requirement that the reference pulse has to be well separated from the data-modulated pulse as in a conventional TR system. With that scheme, data rate is substantially increased, especially in a long multipath channel, and better detection performance of the receiver is achieved even if IPI is present in the system. For low cost and high flexibility, this paper considers practical digital implementation of the receiver. Impact of using a low resolution analog-to-digital converter is investigated. Joint performance of template estimation and symbol detection is also studied.

1. INTRODUCTION

As an ideal candidate for high-rate short-range wireless communication links, ultra-wideband (UWB) technology has caught a lot of attention recently [1]. However, there are still great design challenges in realizing its potentials. Conventional UWB impulse radio correlates the received signal with a local template. But distortions to these extremely short transmitted pulses by transmitter antennas, multipath and receiver antennas are non-negligible. Therefore, the signal waveform is unknown to the receiver. Applying a pre-assumed template leads to suboptimal receivers. Also, estimation of multipath channels and pulse level synchronization are difficult tasks in the context of UWB due to the facts that the transmitted pulse duration is in the order of sub-nanoseconds and multipath components are very rich [2], although high rate sampling makes channel estimation possible by sacrificing low complexity [3]. To overcome these difficulties, transmitted reference (TR) technique is applied to UWB systems with demonstrated demodulation capability in unknown multipath channels [4], [5], [6], [7]. In this scheme, the delay of the information-bearing pulse is designed to be larger than the channel spread such that the reference pulse does not interfere with the information-bearing pulse after multipath propagation [4]. However, that delay inevitably sacrifices data rate for good performance, especially in a long multipath channel [8]. In [9], this constraint is removed in the TR modulation design and corresponding reliable data detection schemes are developed to tackle inter-pulse interference (IPI). Both low complexity mean-based approaches and optimal ML approaches are proposed therein.

Prepared through collaborative participation in the Communications and Networks Consortium sponsored by the U. S. Army Research Laboratory under the Collaborative Technology Alliance Program, Cooperative Agreement DAAD19-01-2-0011. The U. S. Government is authorized to reproduce and distribute reprints for Government purposes notwithstanding any copyright notation thereon.

Although receivers in [9] can be partially implemented using analog circuits, digital implementation is of great interest because it offers many advantages as in conventional narrow band systems, such as low cost and high flexibility. Some researchers have begun to consider digital architectures in UWB systems [10], [11], [12], [13], [14]. Unlike in narrow band systems, analog-to-digital converters (ADCs) constitute major technical difficulties in UWB systems because ADC is required to achieve a few giga samples per second according to the Nyquist sampling theorem. The state-of-the-art ADC is reported to have only 6 bits of resolution at 1.3 GSamples/s [15]. Consequently, a practical way for implementing UWB digital receivers is to apply low resolution ADCs. In [13], the authors studied monobit receivers with different ADCs and showed effective monobit receivers require oversampling. We consider ADCs with finite resolution and examine their effects on digital receivers proposed in [9]. Different from [14], we perform joint performance analysis of estimation and detection in TR systems with IPI. In addition, because our current focus is low resolution ADC, we need to accurately model the quantization error instead of assuming it is uniformly distributed as in [14].

This paper only considers binary pulse amplitude modulation (PAM) without repetition of a symbol by multiple frames. But discussions can be easily extended to arbitrary modulation levels, multiple frames and pulse position modulation (PPM) based UWB systems.

2. RECEIVER STRUCTURE

In a PAM-TR UWB system, two pulses are transmitted within each symbol duration of T_s seconds. The second pulse is data modulated by PAM and delayed T_d seconds from the first reference pulse. Denote the pulse used in the system by $p(t)$ with duration T_p and the binary PAM symbol by $A_n \in \{\pm 1\}$. The transmitted signal with power P can be described by [5]

$$s(t) = \sqrt{P/2} \sum_n [p(t - nT_s) + A_n p(t - nT_s - T_d)]. \quad (1)$$

Reasonably assume $T_d > T_p$ and $T_d + T_p < T_s$, meaning the first and second pulses do not interfere each other before propagation through a channel. However, this no longer holds at the receiver after the transmitted signal passes through a multipath channel. If we denote the response of a multipath channel by $g(t)$ and apply the matched filter $p(-t)$ first at the receiver, then the received signal becomes

$$r(t) = \sum_n [h(t - nT_s) + A_n h(t - nT_s - T_d)] + v(t), \quad (2)$$

where $h(t) = \sqrt{P/2}p(t) \star g(t) \star p(-t)$ is the dispersed waveform with energy $E_b/2$, \star denotes convolution, and $v(t)$ represents white Gaussian noise with zero mean and double-sided power spectral density $N_0/2$. We assume the physical channel is quasi-static, implying it does not change over a transmission burst but will change from burst to burst. Without loss of generality, suppose $h(t)$ has support in $(0, T_h)$ and $T_h + T_d < T_s$ to avoid intersymbol interference (ISI). However, all later discussions can be generalized to a situation with ISI.

Our receiver structure is depicted in Fig. 1. After the receiving antenna, the low noise amplifier and the matched filter, the received signal is sampled and digitized by ADC. Then we can process the resulting digital signal to detect transmitted information symbols. The ADC samples the signal $r(t)$ every T_t seconds at a b -bit precision. T_t is related to T_d by $T_d = LT_t$ with integer L . Under such sampling, the number of samples in one symbol interval becomes $K = \lceil \frac{T_s}{T_t} \rceil$ where $\lceil \cdot \rceil$ denotes integer ceiling. The maximum multipath channel span is upper bounded by $q = \lceil \frac{T_h}{T_t} \rceil$ units. Accordingly, all q channel coefficients are stacked in a vector $\mathbf{h} = [h_1, \dots, h_q]^T$. We define discrete-time digital samples in the n th symbol interval $r(n, k) = r(t)|_{t=nT_s+kT_t} + e(n, k)$ for $k = 1, \dots, K$. Here, the quantization error has been modelled as additive noise $e(n, k)$. If all these samples are collected in a vector \mathbf{r}_n , then according to [9] and incorporating quantization noise, it becomes

$$\begin{aligned} \mathbf{r}_n &= \begin{bmatrix} \mathbf{h} \\ \mathbf{0}_{(K-q) \times 1} \end{bmatrix} + A_n \begin{bmatrix} \mathbf{0}_{L \times 1} \\ \mathbf{h} \\ \mathbf{0}_{(K-L-q) \times 1} \end{bmatrix} + \mathbf{v}_n + \mathbf{e}_n \\ &= \mathbf{C}_n \mathbf{h} + \mathbf{v}_n + \mathbf{e}_n \end{aligned} \quad (3)$$

where \mathbf{v}_n contains discrete-time noise components, \mathbf{e}_n is the quantization noise vector,

$$\mathbf{C}_n = \begin{bmatrix} \mathbf{I}_q \\ \mathbf{0}_{(K-q) \times q} \end{bmatrix} + A_n \begin{bmatrix} \mathbf{0}_{L \times q} \\ \mathbf{I}_q \\ \mathbf{0}_{(K-L-q) \times q} \end{bmatrix}, \quad (4)$$

and \mathbf{I}_q is an identity matrix of dimension q .

In order to achieve reliable detection, we want to extract a clean reference waveform from the noisy digital signal first. Then we can apply a correlation receiver to detect transmitted information symbols. For low complexity, we consider the first order statistic of \mathbf{r}_n to estimate \mathbf{h} as described in [9]. It is observed from (3) that both A_n and \mathbf{v}_n have zero mean, thus we have $E\{\mathbf{r}_n(1:q)\} = \mathbf{h}$ if no quantization noise. Here a Matlab notation to extract elements from a vector has been introduced. That implies the mean completely captures the channel response. Even with quantization noise, we can still build a mean-based estimator based on N received data vectors

$$\hat{\mathbf{h}} = N^{-1} \sum_{n=1}^N \mathbf{r}_n(1:q). \quad (5)$$

Because of the existence of quantization error in the output of ADC, additional error due to quantization is introduced in the above channel estimator besides the error due to finite sample size studied in [9]. It thus leads to further performance degradation. We will quantify such a degradation and discuss associated influencing factors in the next section.

Once \mathbf{h} is obtained, an estimate of A_n can be obtained using the low-complexity correlation receiver as [9]

$$\hat{A}_n = \text{sign}(\hat{\mathbf{h}}^T \mathbf{y}_n). \quad (6)$$

Here, \mathbf{y}_n is the received data vector after inter pulse interference is removed

$$\mathbf{y}_n = \mathbf{r}_n(L+1:L+q) - [\hat{h}_{L+1}, \dots, \hat{h}_q, \mathbf{0}_{1 \times L}]^T.$$

3. PERFORMANCE STUDY

In this section, we study performance of the above proposed digital receiver with practical ADC. We will first obtain some statistics of quantization noise and then analyze channel estimation error and probability of symbol detection error sequentially.

3.1. Quantization Noise

In the literature, quantization noise is commonly assumed to be uniformly distributed and uncorrelated with the analog input [14]. But in the context of UWB systems, this assumption becomes questionable. Because high resolution ADCs with several GHz sampling rate is far from being practical, the major condition to justify these assumptions becomes invalid [16]. Therefore, we need accurately formulate the distribution of quantization noise. Assume the ADC is not overloaded and has symmetric full scale from $-V_m$ to V_m . We only consider a midriser ADC, which means it has an even number of output levels and does not contain a zero in its output. Then quantization step $\Delta = 2V_m/(2^b - 1)$. Suppose the ADC uses a roundoff quantizer. The probability density function (PDF) of quantization error e given input x is [16]

$$f_e(e) = \begin{cases} \frac{1}{\Delta} + \frac{1}{\Delta} \sum_{k \neq 0} (-1)^k \phi_x\left(\frac{2\pi k}{\Delta}\right) \exp\left(\frac{j2\pi k e}{\Delta}\right), & -\Delta/2 \leq e < \Delta/2 \\ 0, & \text{otherwise.} \end{cases} \quad (7)$$

$\phi_x(\omega)$ is the characteristic function of input analog signal, given by

$$\phi_x(\omega) = \int_{-\infty}^{\infty} f_x(x) \exp(jx\omega) dx. \quad (8)$$

From (3), we know the analog signal before quantization $\mathbf{x}_n = \mathbf{C}_n \mathbf{h} + \mathbf{v}_n$ is conditional Gaussian on A_n with conditional mean $\boldsymbol{\mu}_1$ or $\boldsymbol{\mu}_2$ and covariance matrix $\sigma_v^2 \mathbf{I}_K$. $\boldsymbol{\mu}_1$ and $\boldsymbol{\mu}_2$ are two possible vectors of $\mathbf{C}_n \mathbf{h}$ corresponding to $A_n = \pm 1$. Because A_n takes two values with equal probability, we obtain

$$\phi_x(\omega) = \frac{1}{2} \exp(j\omega \boldsymbol{\mu}_1 - \frac{1}{2} \omega^2 \sigma_v^2) + \frac{1}{2} \exp(j\omega \boldsymbol{\mu}_2 - \frac{1}{2} \omega^2 \sigma_v^2), \quad (9)$$

where μ_1 and μ_2 are corresponding elements in $\boldsymbol{\mu}_1$ and $\boldsymbol{\mu}_2$. Substituting (9), (7) becomes

$$f_e(e) = \begin{cases} \frac{1}{\Delta} \left[1 + \sum_{k=1}^{\infty} \left(\cos\left(\frac{2\pi k(e+\mu_1)}{\Delta}\right) + \cos\left(\frac{2\pi k(e+\mu_2)}{\Delta}\right) \right) \right. \\ \quad \left. (-1)^k \exp\left(-\frac{2\pi^2 k^2 \sigma_v^2}{\Delta^2}\right) \right], & -\Delta/2 \leq e < \Delta/2 \\ 0, & \text{otherwise.} \end{cases} \quad (10)$$

We want to point out the above PDF subsumes the special case that input signal is Gaussian distributed with mean μ and variance σ_v^2 . The PDF can be directly obtained by setting $\mu_1 = \mu_2 = \mu$.

Next using (10), we can calculate the mean and correlation of the quantization error as follows:

$$\begin{aligned} E[e] &= \sum_{k \neq 0} \frac{\Delta}{2\pi k} \left[\sin\left(\frac{2\pi k \mu_1}{\Delta}\right) + \sin\left(\frac{2\pi k \mu_2}{\Delta}\right) \right] \\ &\quad \times \exp\left(-\frac{2\pi^2 k^2 \sigma_v^2}{\Delta^2}\right), \end{aligned} \quad (11)$$

$$E[e^2] = \frac{\Delta^2}{12} + \sum_{k \neq 0} \frac{\Delta^2}{2\pi^2 k^2} \left[\cos\left(\frac{2\pi k \mu_1}{\Delta}\right) + \cos\left(\frac{2\pi k \mu_2}{\Delta}\right) \right] \times \exp\left(-\frac{2\pi^2 k^2 \sigma_v^2}{\Delta^2}\right). \quad (12)$$

With (11), it is clear that the mean of quantization noise generally is nonzero because $\mu_{\{1,2\}}$ are nonzero. The smaller number of bits the quantizer has or the smaller the background noise is, the bigger the mean is. This counter-intuitive result will be further described in Section 3.2, as well as in our simulation results in Section 4.

Another conventional assumption we think inappropriate in UWB systems is that input signal is uncorrelated with quantization noise. The cross-correlation can be derived as in [16]

$$E[xe] = \frac{\Delta}{2\pi} \sum_{k \neq 0} \left(\frac{\mu_1}{k} \sin\left(\frac{2\pi k \mu_1}{\Delta}\right) + \frac{2\pi \sigma_v^2}{\Delta} \cos\left(\frac{2\pi k \mu_1}{\Delta}\right) \right) + \frac{\mu_2}{k} \sin\left(\frac{2\pi k \mu_2}{\Delta}\right) + \frac{2\pi \sigma_v^2}{\Delta} \cos\left(\frac{2\pi k \mu_2}{\Delta}\right) \times \exp\left(-\frac{2\pi^2 k^2 \sigma_v^2}{\Delta^2}\right). \quad (13)$$

When σ_v is small and the number of bits of ADC is small, the dependence between input signal and quantization noise becomes more obvious.

Because x_n are independent at different time n , e_{n_1} and e_{n_2} are also independent for $n_1 \neq n_2$. However, different elements in e_n are dependent because they are related to the same A_n . For a given A_n , $e_n(i_1)$ and $e_n(i_2)$ are independent as $v_n(i_1)$ and $v_n(i_2)$ are independent if $i_1 \neq i_2$. Thus, cross-correlation $E[e_n(i_1)e_n(i_2)]$ of the i_1 -th element and i_2 -th element in e_n is given by

$$E[e_n(i_1)e_n(i_2)] = \frac{\Delta^2}{2\pi^2} \left[\sum_{k_1, k_2 \neq 0} \frac{1}{k_1 k_2} \sin\left(\frac{2\pi k_1 \mu_1(i_1)}{\Delta}\right) \times \sin\left(\frac{2\pi k_2 \mu_1(i_2)}{\Delta}\right) \exp\left(-\frac{2\pi^2 \sigma_v^2 (k_1^2 + k_2^2)}{\Delta^2}\right) \right] + \frac{\Delta^2}{2\pi^2} \left[\sum_{k_1, k_2 \neq 0} \frac{1}{k_1 k_2} \sin\left(\frac{2\pi k_1 \mu_2(i_1)}{\Delta}\right) \times \sin\left(\frac{2\pi k_2 \mu_2(i_2)}{\Delta}\right) \exp\left(-\frac{2\pi^2 \sigma_v^2 (k_1^2 + k_2^2)}{\Delta^2}\right) \right]. \quad (14)$$

Similarly, cross-correlation between input and quantization noise at the same n is obtained

$$E[x_n(i_1)e_n(i_2)] = \frac{\Delta}{2\pi} \mu_1(i_1) \sum_{k \neq 0} \frac{1}{k} \sin\left(\frac{2\pi k \mu_1(i_2)}{\Delta}\right) \times \exp\left(-\frac{2\pi^2 k^2 \sigma_v^2}{\Delta^2}\right) + \frac{\Delta}{2\pi} \mu_2(i_1) \sum_{k \neq 0} \frac{1}{k} \sin\left(\frac{2\pi k \mu_2(i_2)}{\Delta}\right) \times \exp\left(-\frac{2\pi^2 k^2 \sigma_v^2}{\Delta^2}\right). \quad (15)$$

3.2. Channel Estimation Performance

Our waveform estimator is constructed by exploring statistics of N digital random vectors. Its performance is affected by noise, quantization error and data length. For notational convenience, we define

$$\mathbf{x}_u = \mathbf{x}_n(1 : q), \quad \mathbf{x}_l = \mathbf{x}_n(L+1 : L+q),$$

$$\mathbf{e}_u = \mathbf{e}_n(1 : q), \quad \mathbf{e}_l = \mathbf{e}_n(L+1 : L+q),$$

$$\mathbf{v}_l = \mathbf{v}_n(L+1 : L+q),$$

where subscripts ‘‘u’’ and ‘‘l’’ represent upper and lower sub-vectors of a vector. With (3), the estimator (5) can be rewritten as

$$\hat{\mathbf{h}} = N^{-1} \sum_{n=1}^N (\mathbf{x}_u + \mathbf{e}_u) = \mathbf{h} + N^{-1} \sum_{n=1}^N (A_n \mathbf{J}^L \mathbf{h} + \mathbf{v}_u + \mathbf{e}_u), \quad (16)$$

where matrix \mathbf{J} of size $q \times q$ represents a shift-down operator with all elements to be zero except the first lower sub-diagonal to be 1's. Then estimation error

$$\delta \mathbf{h} = \hat{\mathbf{h}} - \mathbf{h} = \delta \mathbf{h}_f + \tilde{\mathbf{e}}, \quad (17)$$

where $\delta \mathbf{h}_f = N^{-1} \sum_{n=1}^N (A_n \mathbf{J}^L \mathbf{h} + \mathbf{v}_u)$ represents the channel estimation error if the quantizer has full resolution (infinite number of bits), and $\tilde{\mathbf{e}} = N^{-1} \sum_{n=1}^N \mathbf{e}_u$ is a newly defined averaged quantization noise vector. Since the covariance matrix of $\delta \mathbf{h}_f$ is derived in [9] as:

$$\mathbf{\Pi} = E\{\delta \mathbf{h}_f \delta \mathbf{h}_f'\} = \frac{1}{N} (\mathbf{J}^L \mathbf{h} \mathbf{h}' \mathbf{J}^{-L} + \sigma_v^2 \mathbf{I}_q), \quad (18)$$

covariance matrix of $\delta \mathbf{h}$ is obtained as

$$\begin{aligned} \text{COV} &= E\{\delta \mathbf{h} \delta \mathbf{h}'\} = \mathbf{\Pi} + \frac{1}{N} (E\{\mathbf{x}_u \mathbf{e}_u'\} - \mathbf{h} E\{\mathbf{e}_u'\} \\ &+ E\{\mathbf{e}_u \mathbf{x}_u'\} - E\{\mathbf{e}_u\} \mathbf{h}' + E\{\mathbf{e}_u \mathbf{e}_u'\}) \\ &+ \left(1 - \frac{1}{N}\right) E\{\mathbf{e}_u\} E\{\mathbf{e}_u'\}, \end{aligned} \quad (19)$$

where $'$ denotes transpose operation. Comparing (18) with (19), we can clearly see the additional errors incurred due to quantization by the mean and variance of quantization noise, and cross-correlation between input and quantization noise. Although we can reduce the effect of quantization error by increasing N to some extent, there is a limit in such an improvement because of the last term in (19), which does not decrease with respect to N . An mean-square-error (MSE) floor appears when N is above a certain value. However, the error floor will diminish if the noise power σ_v^2 is big or the resolution of the quantizer is high.

3.3. Detection Performance

Without loss of generality, we first assume information ‘‘1’’ is transmitted, i.e., $A_n = 1$. With (3), (6) and (17), the decision statistic can be rewritten as

$$\begin{aligned} \hat{\mathbf{h}}_n' &= \hat{\mathbf{h}}' (A_n \mathbf{h} + \mathbf{J}^{-L} \mathbf{h} + \mathbf{v}_l + \mathbf{e}_l - \mathbf{J}^{-L} \hat{\mathbf{h}}) \\ &= (\mathbf{h} + \delta \mathbf{h}_f + \tilde{\mathbf{e}})' (A_n \mathbf{h} + \mathbf{v}_l + \mathbf{e}_l - \mathbf{J}^{-L} \delta \mathbf{h}_f - \mathbf{J}^{-L} \tilde{\mathbf{e}}) \\ &= A_n \mathbf{h}' \mathbf{h} + \xi_n, \end{aligned} \quad (20)$$

where all noise terms are lumped into ξ_n . According to the central limit theorem, it is reasonable to assume ξ_n is a Gaussian random variable with conditional mean and conditional variance as

$$m_\xi = \mathbf{h}'\mathbf{m} - \mathbf{h}'\mathbf{J}^{-L}\tilde{\mathbf{m}} + \mathbf{h}'\tilde{\mathbf{m}} + \tilde{\mathbf{m}}'\mathbf{m} - \text{tr}\left(\mathbf{J}^{-L}(\boldsymbol{\Psi} + \boldsymbol{\Psi}' + \tilde{\boldsymbol{\Theta}} + \boldsymbol{\Pi})\right), \quad (21)$$

$$\begin{aligned} \sigma_\xi^2 &\approx \sigma_v^2\mathbf{h}'\mathbf{h} + \mathbf{h}'(\boldsymbol{\Pi} + \mathbf{J}^{-L}\boldsymbol{\Pi}\mathbf{J}^L - 2\mathbf{J}^{-L}\boldsymbol{\Pi})\mathbf{h} + \sigma_v^2\text{tr}(\boldsymbol{\Pi}) \\ &+ \mathbf{h}'(\boldsymbol{\Phi} + \tilde{\boldsymbol{\Phi}} + 2\boldsymbol{\Omega} + \mathbf{J}^{-L}\tilde{\boldsymbol{\Phi}}\mathbf{J}^L - 2\mathbf{J}^{-L}\tilde{\boldsymbol{\Phi}})\mathbf{h} \\ &+ \sigma_v^2\text{tr}(\tilde{\boldsymbol{\Theta}}) + 2\sigma_v^2\mathbf{h}'\tilde{\mathbf{m}} + \text{tr}(\boldsymbol{\Theta}\tilde{\boldsymbol{\Theta}}) - (\tilde{\mathbf{m}}'\mathbf{m})^2 \\ &+ 2\mathbf{h}'(\boldsymbol{\Omega}' + \boldsymbol{\Omega} + \tilde{\boldsymbol{\Phi}})\tilde{\mathbf{m}} + 2\mathbf{h}'(\tilde{\boldsymbol{\Phi}} - \mathbf{J}^{-L}\tilde{\boldsymbol{\Phi}})\mathbf{m} \\ &+ 2\text{tr}(\tilde{\boldsymbol{\Theta}}\boldsymbol{\Omega}) + 2\mathbf{h}'(\boldsymbol{\Psi} + \mathbf{J}^{-L}\boldsymbol{\Psi}\mathbf{J}^L - \mathbf{J}^{-L}\boldsymbol{\Psi} - \mathbf{J}^{-L}\boldsymbol{\Psi}')\mathbf{h} \\ &+ 2\sigma_v^2\text{tr}(\boldsymbol{\Psi}) + \text{tr}(\boldsymbol{\Pi}\boldsymbol{\Theta} + 2\boldsymbol{\Psi}'\boldsymbol{\Theta}) \\ &+ 2\mathbf{h}'(\boldsymbol{\Pi} + \boldsymbol{\Psi} + \boldsymbol{\Psi}' - \mathbf{J}^{-L}\boldsymbol{\Pi} - \mathbf{J}^{-L}\boldsymbol{\Psi} - \mathbf{J}^{-L}\boldsymbol{\Psi}')\mathbf{m} \\ &+ 2\text{tr}(\boldsymbol{\Pi}\boldsymbol{\Omega} + \boldsymbol{\Omega}\boldsymbol{\Psi}' + \boldsymbol{\Omega}\boldsymbol{\Psi}), \end{aligned} \quad (22)$$

where

$$\begin{aligned} \mathbf{m} &= E\{e_l|A_n = 1\}, \tilde{\mathbf{m}} = E\{\tilde{e}\}, \\ \boldsymbol{\Theta} &= E\{e_l e_l'|A_n = 1\}, \tilde{\boldsymbol{\Theta}} = E\{\tilde{e}\tilde{e}'\}, \\ \boldsymbol{\Phi} &= E\{(e_l - \mathbf{m})(e_l - \mathbf{m})'|A_n = 1\}, \\ \tilde{\boldsymbol{\Phi}} &= E\{(\tilde{e} - \tilde{\mathbf{m}})(\tilde{e} - \tilde{\mathbf{m}})'\}, \\ \boldsymbol{\Omega} &= E\{x_l e_l'|A_n = 1\} - (\mathbf{h} + \mathbf{J}^{-L}\mathbf{h})\mathbf{m}', \\ \boldsymbol{\Psi} &= N^{-1}(E\{x_l \tilde{e}'\} - \mathbf{h}\tilde{\mathbf{m}}'). \end{aligned}$$

We have approximated σ_ξ^2 by keeping those terms up to the second order statistics of $\delta\mathbf{h}_f$, \mathbf{v}_l , \tilde{e} and e_l .

Similarly, we can obtain the mean and variance conditioned on $A_n = -1$. Theoretically, they are different from those in (21) and (22). But from our simulation, they are close to each other. Thus, we approximate the average bit error rate (BER) \bar{P}_e by

$$\begin{aligned} \bar{P}_e &= \frac{1}{2}P_{e|A_n=1} + \frac{1}{2}P_{e|A_n=-1} \\ &\approx P_{e|A_n=1} = Q\left(\frac{\mathbf{h}'\mathbf{h} + m_\xi}{\sigma_\xi}\right), \end{aligned} \quad (23)$$

where $Q(\cdot)$ is the Q -function defined as $Q(x) = \int_x^\infty \frac{1}{\sqrt{2\pi}} e^{-\frac{t^2}{2}} dt$.

To gain more insight into the detection performance characterized by (21)-(23), we will discuss two special cases where BER results can be simplified.

A. Full resolution quantizer: No quantization error exists in this case. (21) and (22) reduce to

$$m_\xi = -\text{tr}\left(\mathbf{J}^{-L}\boldsymbol{\Pi}\right), \quad (24)$$

$$\sigma_\xi^2 \approx \sigma_v^2\mathbf{h}'\mathbf{h} + \mathbf{h}'(\boldsymbol{\Pi} + \mathbf{J}^L\boldsymbol{\Pi}\mathbf{J}^{-L} - 2\mathbf{J}^{-L}\boldsymbol{\Pi})\mathbf{h} + \sigma_v^2\text{tr}(\boldsymbol{\Pi}). \quad (25)$$

B. Large sample size: In this case, those terms inversely proportional to N can be ignored, which include $\boldsymbol{\Pi}$, $\tilde{\boldsymbol{\Phi}}$, $\boldsymbol{\Psi}$. However, $\boldsymbol{\Phi}$, $\boldsymbol{\Theta}$, $\tilde{\boldsymbol{\Theta}}$, $\boldsymbol{\Omega}$ are non-negligible. Consequently, conditional mean and variance become

$$m_\xi = \mathbf{h}'\mathbf{m} - \mathbf{h}'\mathbf{J}^{-L}\tilde{\mathbf{m}} + \mathbf{h}'\tilde{\mathbf{m}} + \tilde{\mathbf{m}}'\mathbf{m} - \text{tr}\left(\mathbf{J}^{-L}\tilde{\boldsymbol{\Theta}}\right), \quad (26)$$

$$\begin{aligned} \sigma_\xi^2 &\approx \sigma_v^2\mathbf{h}'\mathbf{h} + \mathbf{h}'(\boldsymbol{\Phi} + 2\boldsymbol{\Omega})\mathbf{h} \\ &+ \sigma_v^2\text{tr}(\tilde{\boldsymbol{\Theta}}) + 2\sigma_v^2\mathbf{h}'\tilde{\mathbf{m}} + \text{tr}(\boldsymbol{\Theta}\tilde{\boldsymbol{\Theta}}) - (\tilde{\mathbf{m}}'\mathbf{m})^2 \\ &+ 2\mathbf{h}'(\boldsymbol{\Omega}' + \boldsymbol{\Omega})\tilde{\mathbf{m}} + 2\text{tr}(\tilde{\boldsymbol{\Theta}}\boldsymbol{\Omega}). \end{aligned} \quad (27)$$

It is clear that increase of N can not completely counter the quantization error although it can reduce its effect to a certain extent.

4. SIMULATIONS

We adopt normalized second derivative of Gaussian pulse with duration of $0.7ns$ as transmitted monopulse. T_s is $51ns$ and T_d is $10ns$. Discrete-time multipath channels are generated using the IEEE UWB CM2 channel model [8] with maximum delay spread $T_h = 40ns$ and time resolution $0.1ns$. About 80% of the multipath energy is beyond the $10ns$ delay window of the information-bearing pulse, causing severe IPI. The maximum quantized output value V_m of the ADC is chosen to be twice as large as the maximum value of transmitted clean signal and $T_t = 0.1ns$. We first test ADCs with different resolution and sample size N . Channel MSE normalized by the number of estimated parameters, i.e. $q^{-1}\|\mathbf{h}\|^{-2}E\{\|\hat{\mathbf{h}} - \mathbf{h}\|^2\}$, is plotted in Fig. 2. It is observed that analytical results are consistent with simulated ones. On the other hand, analysis based on conventional assumptions show some deviation from simulations, especially at high SNR and low resolution. Compared with the full resolution quantizer (i.e., no quantization error), the 1-bit quantizer results in larger MSE. In contrast to unlimited decrease of MSE with increase of N using full resolution ADC, a MSE floor occurs for each finite resolution ADC when N is sufficiently large as predicted by (19). The error floor level and the critical value N at which the floor appears depend on both resolution and SNR.

To have better understanding of the effect of SNR and ADC resolution, we test the channel estimator and detector for fixed $N = 200$. Fig. 3 shows MSE. At higher SNR, differences of channel estimation performance among different resolution ADCs become bigger. This confirms previous analysis that quantization noise is larger at higher SNR. All MSE curves decrease first, then increase, and finally converge. The analytical expression (19) can help us explain such a pattern. Because channel noise dominates MSE in low SNR region, MSE decreases with increase of SNR. On the other hand, quantization noise increases as SNR increases. After certain point, quantization noise will dominate MSE. Then MSE trend reverses and eventually converges. Convergence level is lower with high resolution ADC than that with low resolution ADC. Fig. 4 shows detection performance of our digital receiver. Simulated and analytical BERs are compared at different resolutions. A small gap is observed for a mono-bit receiver, but good agreement for receivers with more than one bit. The mono-bit receiver has worse performance than a full resolution receiver. But a 3-bit receiver can almost attain the same performance as a full resolution receiver. Therefore, three bits are sufficient for our digital receiver to function properly in UWB systems with inter-pulse interference.

5. REFERENCES

- [1] M. D. Benedetto and G. Giancola, *Understanding Ultra Wide Band Radio Fundamentals*. NJ: Prentice Hall, 2004.
- [2] M. Z. Win and R. A. Scholtz, "Characterization of ultra-wide bandwidth wireless indoor channels: a communication-theoretic view," *IEEE J. Selected Areas Commun.*, vol. 20, no. 9, pp. 1613–1627, Dec. 2002.
- [3] Z. Xu, J. Tang, and P. Liu, "Multiuser channel estimation for ultra-wideband systems using up to the second order statistics," *EURASIP*

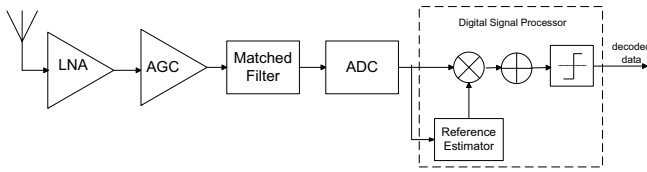


Fig. 1. Block diagram of the digital receiver.

Journal on Applied Signal Processing: Special Issue on UWB - State of the Art, vol. 2005, no. 3, pp. 273–286, Mar. 2005.

- [4] J. D. Choi and W. E. Stark, "Performance of ultra-wideband communications with suboptimal receivers in multipath channels," *IEEE J. Selected Areas Commun.*, vol. 20, no. 9, pp. 1754–1766, Dec. 2002.
- [5] R. T. Hocht and H. W. Tomlinson, "Delay-hopped transmitted reference RF communications," in *Proc. 2002 UWBST*, Baltimore, MD, May 2002, pp. 265–270.
- [6] Y. L. Chao and R. A. Scholtz, "Optimal and suboptimal receivers for ultra-wideband transmitted reference systems," in *Proc. IEEE Globecom*, vol. 2, San Francisco, CA, Dec. 2003, pp. 759–763.
- [7] S. Franz and U. Mitra, "On optimal data detection for UWB transmitted reference systems," in *Proc. IEEE Globecom*, vol. 2, San Francisco, CA, Dec. 2003, pp. 744–748.
- [8] IEEE P802.15 Working Group, "Channel modeling sub-committee report final," IEEE P802.15-02/490r1-SG3a, Feb. 2003.
- [9] Z. Xu, B. Sadler, and J. Tang, "Data detection for UWB transmitted reference systems with inter-pulse interference," in *Proc. of ICASSP'05*, Philadelphia, Mar. 2005.
- [10] S. Hoyos, B. M. Sadler, and G. R. Arce, "High-speed A/D conversion for ultra-wideband signals based on signal projection over basis functions," in *Proc. of ICASSP*, Montreal, Quebec, Canada, May 2004.
- [11] D. Dabeer and U. Madhow, "Detection and interference suppression for ultra-wideband signaling with analog processing and one bit A/D," in *Proc. of Asilomar*, vol. 2, Monterey, CA, Nov. 2003, pp. 1766–1770.
- [12] W. Namgoong, "A channelized digital ultra-wideband receiver," *IEEE Trans. Wireless Commun.*, vol. 3, no. 5, pp. 502–510, May 2003.
- [13] S. Hoyos, B. Sadler, and G. Arce, "Mono-bit digital receivers for ultra-wideband communications," *IEEE Trans. Wireless Commun.*, (in press).
- [14] P. Newaskar, R. Blazquez, and A. Chandrakasan, "A/D precision requirements for an ultra-wideband radio receiver," in *Proc. of IEEE Workshop on Signal Processing Sys.*, Oct. 2002, pp. 270–275.
- [15] M. Choi and A. A. Abidi, "A 6b 1.3 gsamples/s A/D converter in 0.35 μm CMOS," in *Proc. IEEE Int. Solid-State Circuits Conf.*, vol. 438, 2001, pp. 126–127.
- [16] A. B. Sripad and D. L. Snyder, "A necessary and sufficient condition for quantization errors to be uniform and white," *IEEE Trans. Acoust., Speech, Signal Processing*, vol. ASSP-25, no. 5, pp. 442–448, Oct. 1977.

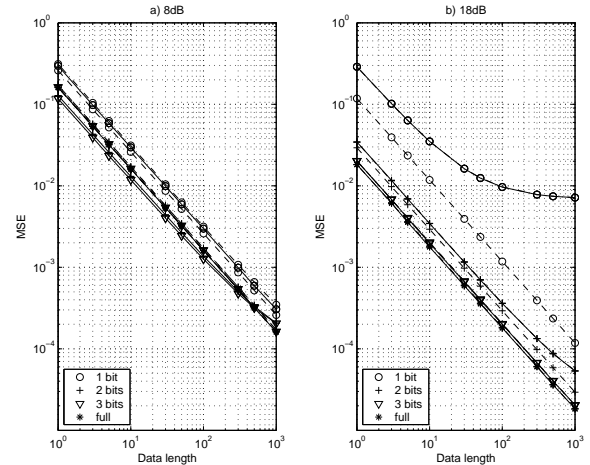


Fig. 2. Normalized MSE with respect to data length. Experimental results: solid lines; analytical results: dash-dotted lines; analytical results based on conventional assumptions: dashed lines.

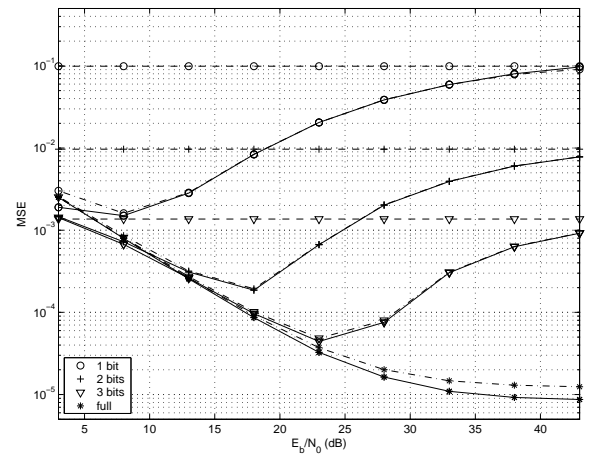


Fig. 3. MSE with respect to SNR and ADC resolution. Experimental results: solid lines; analytical results: dash-dotted lines; convergence levels: dashed lines.

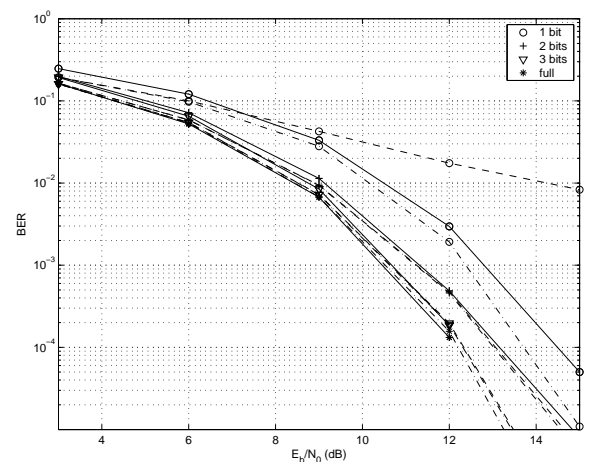


Fig. 4. Detection performance with different resolution ADC at different SNR. Experimental results: solid lines; analytical results: dash-dotted lines; analytical results based on conventional assumptions: dashed lines.